Neural Comput & Applic (2005) 14: 1–10
DOI 10.1007/s00521-004-0433-0

ORIGINAL ARTICLE

Yu-Len Huang

Wavelet-based image interpolation using multilayer perceptrons

Received: 19 April 2004 / Accepted: 13 May 2004 / Published online: 25 August 2004

Abstract Changing the resolution of digital images and video is needed image processing systems. In this paper, we present nonlinear interpolation schemes for still image resolution enhancement. The proposed neural network interpolation method is based on wavelet reconstruction. With the wavelet decomposition, the image signals can be divided into several time–frequency portions. In this work, the wavelet decomposition signal is used to train the neural networks. The pixels in the low-resolution image are used as the input signal of the neural network to estimate all the wavelet sub-images of the corresponding high-resolution image. The image of increased resolution is finally produced by the synthesis procedure of wavelet transform. In the simulation, the proposed method obtains much better performance than other traditional methods. Moreover, the easy implementation and high flexibility of the proposed algorithm also make it applicable to various other related problems.

Keywords Interpolation · Image resampling · Neural network · Wavelet transform · Subband filtering

1 Introduction

Interpolation is the process of estimating the intermediate sample values of a continuous function from known discrete sample values and is used extensively in digital image processing to magnify images and correct spatial distortions. Image interpolation is used for several different purposes, such as image resolution enhancement, multiresolution pyramidal compressing, position computing for rotated image pixels, etc. An efficient interpolation method is essential for digital image processing. Sampling theory dictates that a band-limited analog image can be perfectly reconstructed from its discrete samples if it is sampled at a frequency above the Nyquist rate. An ideal low-pass filter can provide the reconstruction of the image. However, the ideal low-pass filter is not attainable and many approximated interpolation techniques do not give satisfactory performance.

Many linear and nonlinear interpolation techniques have been proposed for image zooming. In the linear methods, the nearest-neighbor, bilinear, cubic B-spline [1] and cubic convolution interpolation methods [2–4] are widely used to increase the resolution of images. Both the nearest-neighbor and bilinear methods provide the interpolation function with a very small computation time. However, these methods cause conspicuous annoying artifacts. Although the cubic interpolation algorithms can reduce the annoying effects, it always blurred the reconstructed image and produced some ringing effects in the edge regions. With the rapid increase in available computing power, the nonlinear techniques for image interpolation have received increasing attention. Median filtering interpolation methods [5] preserve approximately the sharpness of isolated image transitions. However, these methods are difficult to prevent the blurring effects in the interpolated image. Because the characteristics of the edges in a digital image can be reserved for many scales of resolution and the edges are always important for human vision, most of the nonlinear interpolation algorithms tend to focus on the edge information. In edge preserving interpolation methods [6–11], the local edge structure of the original image is preserved to prevent the blurring and blocking effects. These techniques determine the edge localization or classification by exploiting an edge fitting technique within small overlapping windows of the original image. We notice that the interpolation schemes utilize different reconstruction rules that are decided by the edge pattern. However, if the window size is larger or the edges in a window are irregular, the implementation will become complex and inefficient, and the schemes will produce poor performance for image resolution enhancement.

Y.-L. Huang
Department of Computer Science and Information Engineering, Tunghai University, 407 Taichung, Taiwan
E-mail: ylhuang@mail.thu.edu.tw
Tel.: +886-4-23590121
Fax: +886-4-23591567

As in [12, 13], the multiresolution interpolation methods exploit the regularity of edges across resolution scales to estimate the high-frequency information. These methods estimate the regularity of edges by measuring the rate of decay of wavelet transform coefficients across scales and attempt to preserve the underlying regularity by extrapolating a new high-frequency sub-image. And then, the high-frequency sub-image is used in high-resolution image reconstruction. Another class of interpolation methods is that based on neural networks. In [14–16], these methods employ the neural networks for interpolation, providing advantages of high speed and good image reproduction quality. We found that the multiresolution and neural network interpolation techniques improve image interpolation. Hence, we present a novel interpolation method of low implementation complexity by the effective combination of the wavelet multiresolution reconstruction and the neural network techniques.

Artificial neural network (ANN) techniques have been applied to solve complex problems in the field of image processing. One class of neural networks, multilayer perceptron (MLP), has been found to be particularly effective for problems that can make use of supervised training [17–19]. An MLP enables to extract higher-order statistics by adding one or more hidden layers. This model has become extremely popular for both classification and prediction. Many details on its implementation and uses are given in [19]. In 1987, Lippmann [20] shows that an MLP with two hidden layers are enough to form arbitrary decision regions. This paper employs the two-hidden-layers MLP model as the predictor to increase image resolution. In the interpolation phase, only the wavelet transform reconstruction is used for increasing the resolution of images. The wavelet decomposition is used to produce training samples for the MLP learning process. The proposed interpolation method exploits the nonlinearity property of the MLP neural network to estimate wavelet sub-images.

The rest of this paper is organized as follows. Section 2 reviews the main features of wavelet transform and the MLP neural networks. Section 3 presents the structure of the MLP interpolation scheme based on wavelet transform and subband decomposition. Experimental results are given in Sect. 4 for the still images and image sequence outside the training set. Finally, the conclusions are drawn in Sect. 5.

2 Wavelets and MLP neural networks

In this paper, the bi-orthogonal wavelet decomposition and reconstruction methods are used for MLP training and interpolation, respectively. The bi-orthogonal wavelet filtering requires a few tapes, unlike standard subband QMF (quadrature mirror filter) filtering. The detailed properties and construction of regular bi-orthogonal wavelet transform are described in [21]. Furthermore, the MLP network, which is the standard neural network model, is also performed in the proposed method. The original description of MLP can be found in [22]. In general, the error back-propagation algorithm reported in [23, 24] is the most widely used and is a powerful learning algorithm for the MLP network. For completeness, we review the concepts of the bi-orthogonal wavelet analysis and the MLP neural networks with learning algorithm in the following sections.

2.1 Bi-orthogonal wavelet transform

In practice, the wavelet transform is implemented with a perfect reconstruction filter bank. The idea is to decompose the image signals into sub-images corresponding to different frequency contents. Let $H(\omega)$ and $G(\omega)$ be the low-pass and high-pass filters of a perfect reconstruction filter bank, respectively. In the one-dimensional (1-D) case with one-level decomposition, the input signal $x[n]$ is filtered by $h[n]$ and $g[n]$. Then, the resulted sub-image signals are down-sampled by a factor of two. For the bi-orthogonal wavelet transform used here, the decomposition procedure takes the form:

$$x_{\mathrm{L}}[n] = \sum_k h[k]x[2n-k] \text{ and}$$
$$x_{\mathrm{H}}[n] = \sum_k g[k]x[2n-k] \tag{1}$$

where $x_{\mathrm{L}}[n]$ and $x_{\mathrm{H}}[n]$ denote the approximation and detailed sub-image signals, respectively. The perfect reconstruction is performed by the complementary synthesis filters $\tilde{h}[n]$ and $\tilde{g}[n]$ as follows:

$$x[n] = \sum_k \tilde{h}[2k-n]x_{\mathrm{L}}[n] + \sum_k \tilde{g}[2k-n]x_{\mathrm{H}}[n] \tag{2}$$

In the two-dimensional (2-D) case, the 1-D decomposition procedure is first applied to each row of an image signal. The decomposition results in two intermediate sub-images. Then, the same procedure is applied to each column of the intermediate sub-images. For a one-level decomposition, this results in four sub-images LL, LH, HL, and HH. In hierarchical wavelet decomposition, the sub-image LL is further decomposed into other four sub-images. Similarly, the reconstruction for the image is done one level at a time by using the 1-D reconstruction procedure. The one-level decomposition and reconstruction of the image is presented in Fig. 1. Based on the wavelet theory, the original image signals can be perfectly reconstructed through the wavelet transform if the sub-images are reserved without any degradation.

2.2 Multilayer perceptron (MLP) model

An MLP model contains one or more hidden layers, and the function of neurons in the hidden layer is to arbitrate between the input and the output of the neural network. First, the input feature vector is fed into the source nodes in the input layer of the neural network. The neurons of the input layer constitute the input signals

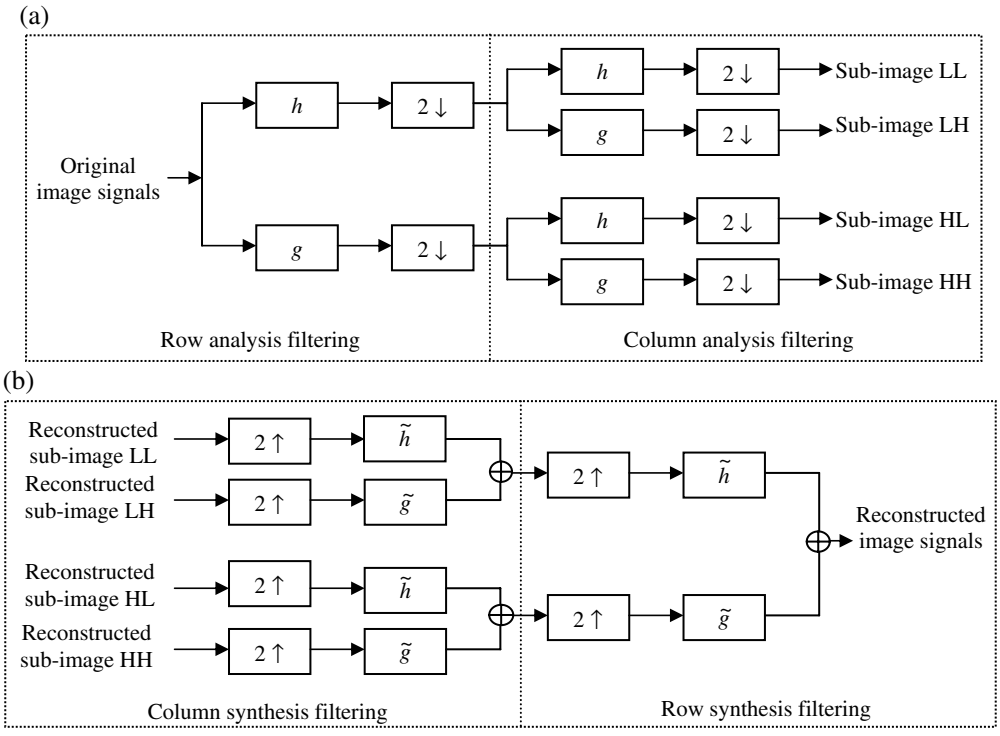

Fig. 1a, b One-level wavelet transform analysis/synthesis. **a** Decomposition. **b** Reconstruction

applied to the neurons of the first hidden layer. The output signals of the hidden layer can be used as inputs to the second hidden layer. Finally, the output layer produces the output result and terminates the neural computing process.

Among the algorithms used to design the MLPs, the back-propagation algorithm is the most popular. In general, there are two different phases in the back-propagation system; the forward phase and the backward phase. In the forward phase, the input signals are computed and passed through the neural network layer by layer. Then, the neurons in the output layer product the output signals of the neural network. In this time, comparing the output response of the neural network with the desired response can generate the error signals. In the backward phase of the back-propagation algorithm, some free parameters can be adjusted by referring the error signals. This work can be used to minimize the distortion of the neural network. We notice that the MLP model has the properties of high learning capability and efficiency. In this work, the back-propagation learning algorithm is iteratively executed for the training set and then produces the synaptic weight vectors. By inputting the final synaptic weight vectors into the MLP, it is used to predict the unknown pixels in our image interpolation schemes.

3 Neural network interpolation using wavelet transform

By using the wavelet decomposition, the solution space of the interpolation problem can be decomposed into its approximation subspace and the complementary detail subspaces. In the frequency domain, this vector space decomposition is equivalent to dividing the spectrum into a high frequency portion and a low frequency portion [25–26]. Empirically, neural networks would obtain better performance when the solution space is reduced. With this, we develop the wavelet MLP interpolation (WMI) scheme that utilizes the property of dividing the image spectrum to augment the interpolation accuracy of the MLP neural networks. WMI does not use the traditional edge classification algorithm to enhance or reserve the detail portion of interpolated image. In general, the 2-D wavelet transform splits the image spectrum into four sub-images LL, LH, HL, and HH. Only the lowest frequency sub-image, LL, is further split into four smaller sub-images. In this paper, we consider the one-level synthesis procedure of wavelet transform for increasing the image resolution by a factor of two.

As shown in Fig. 2, the signal in the overlapping windows of the low-resolution image is used as the input vector of MLP, and then the output signal of the expected wavelet sub-image LL is generated. The same structure is also employed for the reconstruction of the higher-frequency sub-images. Figure 3 shows the relational diagram between the wavelet analysis/synthesis procedure and the MLP modules that are used to estimate the high-resolution image. We employ four MLP modules in the proposed WMI method. Also, all of these four modules are used to estimate the wavelet subband signals. The final synaptic weight vectors ($\mathbf{w}_{LL}$, $\mathbf{w}_{LH}$, $\mathbf{w}_{HL}$, and $\mathbf{w}_{HH}$) for the corresponding wavelet subband image predictors, i.e., MLP_{LL}, MLP_{LH}, MLP_{HL}, and MLP_{HH}, are generated using the back-propagation

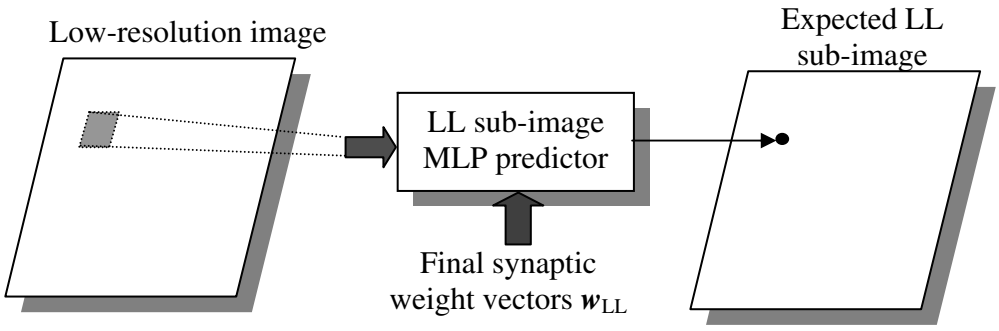

Fig. 2 Block diagram of the LL wavelet sub-image estimation in the WMI scheme

learning algorithm with the images in the training set and its sub-image signals that are generated by the one-level wavelet decomposition. The neural network predictors utilize the low-resolution image signals to estimate the signals in the wavelet subband images of the high-resolution image. Then, the estimated wavelet subband images are performed to compose the interpolated high-resolution image through the 2-D wavelet synthesis operator. The interpolation algorithm for an $M \times N$ low-resolution image with the desired resolution increasing factor of Z is described as follows:

Step 1 Initially store the evaluated final synaptic weight vectors into the corresponding MLP model. Set the width m and height n of the high-resolution image; for

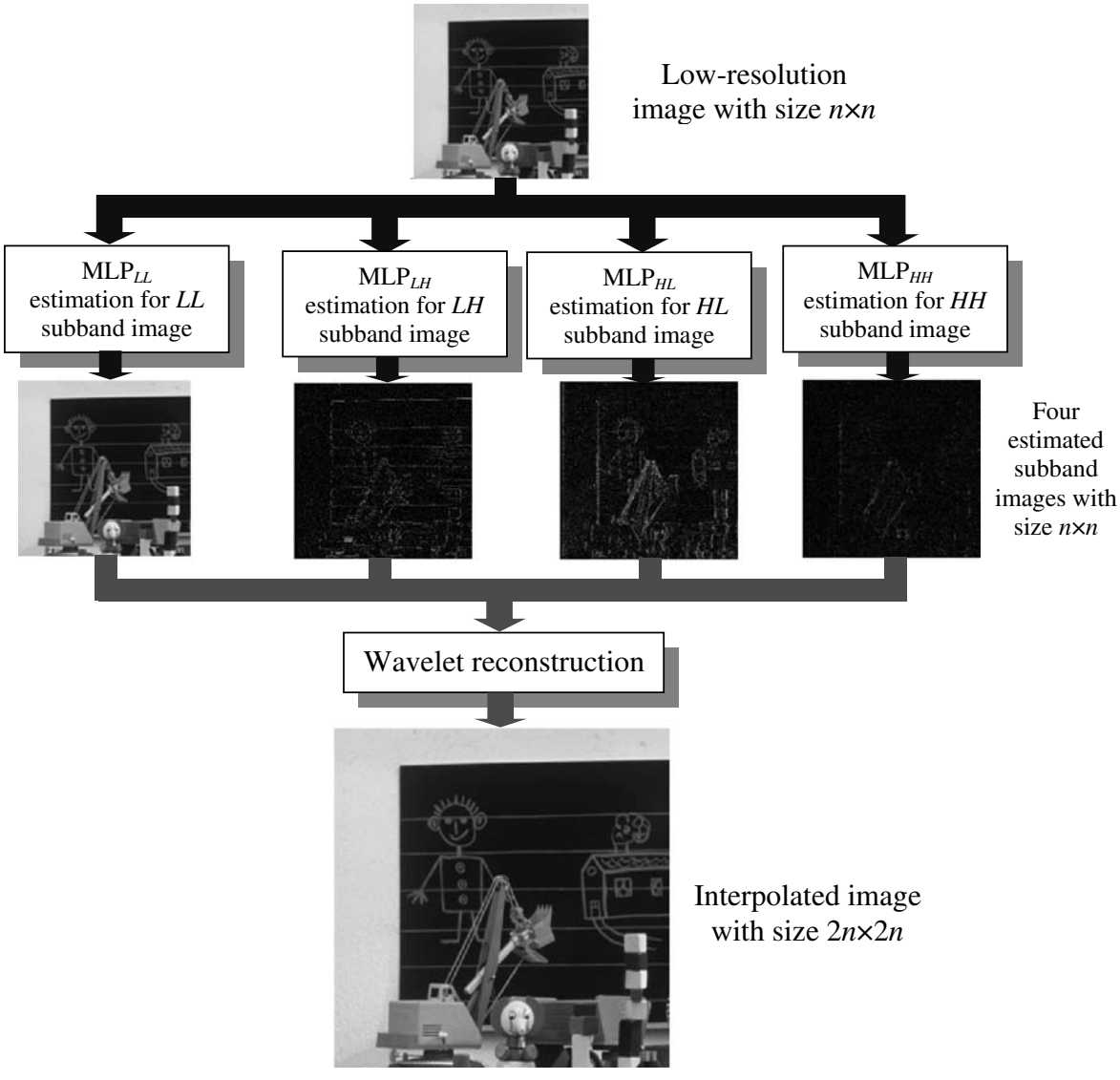

Fig. 3 Block diagram of the WMI algorithm with resolution increasing by a ratio of two

example, $m \leftarrow 2\times M$ and $n \leftarrow 2\times N$, therefore, set $i \leftarrow 1$.
Step 2 The MLP with the synaptic weight vectors $\mathbf{w}_{LL}$ is used to estimate all of the signals in the LL sub-image of the high-resolution image. The signals in the low-resolution image are used as the input vector of the neural network predictor. Similarly, the LH, HL, and HH sub-images can be produced by the corresponding sub-image MLP predictors.
Step 3 Boundary pixels of the LL sub-image, that are incalculable for the LL sub-image predictor, will be filled directly into the low-resolution image in the corresponding position. The incalculable signals in the estimated LH, HL, and HH sub-images are set to 0.
Step 4 Use the 2-D wavelet synthesis procedure to compose the estimated wavelet sub-images. That will result in an $m\times n$ interpolated image with the original resolution increasing by factor 2^i.
Step 5 If $Z/2^i > 1$, then set $i \leftarrow i+1$; set $m \leftarrow 2\times m$ and $n \leftarrow 2\times n$; go to step 2.

In the WMI scheme, the MLP predictors are used to estimate the wavelet sub-images. Furthermore, the WMI scheme supports a progressive interpolation. The reconstructed high-resolution image with acceptable quality can be obtained by only estimating the lowest frequency sub-image. Adding one or more estimated detail sub-images can enhance the fine regions in the image. Furthermore, we find that the proposed algorithm works well for subband reconstruction without any structural modification.

The architecture of the proposed interpolation scheme is simple, redressing easily, and is suitable for hardware design. The MLP neural networks are not only fast, but they are also intrinsically parallel. The Adaptive Connected Network of Adaptive ProcessorS (CNAPS) digital system [27, 28, 29] and the Analog Neural Network Arithmetic and logic unit (ANNA) chip are especially suited to the MLP model. Their simulation results show that both the Adaptive CNAPS digital system [28] and the ANNA chip [29] obtain a speedup factor of 500 over the software implementation on SUN SPARC 1+ workstation. Note that the proposed interpolation scheme only uses one manner of neural network model, i.e., the MLP. Consequently, WMI is potentially fast for the real-time computation of image interpolation.

4 Simulations and results

In the simulations, we use the two-hidden-layer MLP as nonlinear predictors to estimate the spatial signals and the wavelet sub-image in the proposed schemes. The 16-10-5-1 MLP model is used for the WMI scheme. The final synaptic weights of the neural networks are produced by the back-propagation learning algorithm from the training set of five different images; ''Boat'', ''Peppers'', ''Sailboat'', ''Tiffany'', and ''Toys''. The high-resolution images both inside and outside the training set are monochrome still images of size 512×512 pixels with 256 gray levels. The still images are down sampled as low-resolution test images of size 256×256 pixels. The image sequence ''Football'' (352×288 pixels, 30 frames) is also used to evaluate the performance of the proposed approach. To evaluate the performance of the interpolation scheme numerically, the peak signal-to-noise ratio (PSNR) between the two images has been calculated, where the PSNR is defined as:

$$\mathrm{PSNR} = 10\log_{10}\frac{255^2}{\mathrm{MSE}}\ \mathrm{dB} \tag{3}$$

Note that the mean squared error (MSE) for an $n\times n$ image is defined as:

$$\mathrm{MSE} = \left(\frac{1}{n}\right)^2 \sum_{i=1}^{n}\sum_{j=1}^{n}\left(x_{ij} - \hat{x}_{ij}\right)^2 \tag{4}$$

where x_{ij} and $\hat{x}_{ij}$ denote the original and quantized gray levels, respectively.

The proposed interpolation methods and other popular existing interpolation approaches are implemented in this study. Up to now, there has been no such efficient neural-network-based interpolation algorithm proposed. Thus, we compare six interpolation methods: the 2-D bi-directional linear interpolation (denoted by ''Bilinear''), the cubic B-spline interpolation (denoted by ''Cubic''), and the proposed WMI interpolation schemes in the simulations. We also implement a simple version of WMI (denoted by ''$\mathrm{WMI_{LL}}$''), which only uses the estimated sub-image LL to reconstruct the high-resolution image. Moreover, a subband MLP interpolation (denoted by ''SMI'') is constructed by using the same structure as WMI only the analysis/synthesis procedure adopted the subband filter bank. The bi-orthogonal 9/7 filters proposed in [30] are used for the WMI scheme. In the SMI, we use the filter coefficients of the 1-D 32-tap QMF designated as 32C in [31].

Table 1 shows the PSNR values (dB) of the simulation results for the reconstructed still images with the resolution increasing by a factor of two outside the training set. Table 2 and Fig. 4 show the simulation results for interpolated images of the ''Football'' sequence. From the simulation results, we found that the

Table 1 The PSNR values (in dB) of the images with increasing resolution outside the training set

	Bilinear	Cubic	$\mathrm{WMI_{LL}}$	WMI	SMI
Lena	35.7690	36.9666	37.3936	37.8914	38.0228
Family	35.3849	36.9337	37.3418	37.7566	37.9422
F-16	31.4266	33.0702	33.2233	33.4504	33.8368
Baboon	24.4977	25.3423	25.7059	25.8838	25.8470

Table 2 The PSNR values (in dB) of the simulation results for the interpolated images of the "Football" sequence with resolution increasing by a factor of two

Frame no.	Bilinear	Cubic	WMI_{LL}	WMI	SMI
1	29.18	31.70	32.17	32.39	32.40
2	28.61	31.11	31.59	31.84	31.87
3	28.32	30.78	31.22	31.46	31.49
4	27.84	30.26	30.73	30.97	31.02
5	27.49	29.89	30.36	30.66	30.73
6	27.52	29.99	30.46	30.80	30.91
7	27.50	30.16	30.62	30.94	31.04
8	26.98	29.76	30.23	30.57	30.62
9	27.16	30.01	30.54	30.86	30.90
10	26.97	29.66	30.15	30.38	30.43
11	27.18	29.90	30.40	30.67	30.66
12	27.48	30.25	30.72	31.02	31.04
13	27.24	29.93	30.38	30.65	30.72
14	27.09	29.87	30.38	30.60	30.66
15	27.05	29.79	30.29	30.55	30.62
16	27.20	29.93	30.42	30.72	30.78
17	26.80	29.48	29.95	30.19	30.27
18	26.08	28.81	29.28	29.56	29.66
19	25.91	28.65	29.14	29.37	29.44
20	25.98	28.84	29.37	29.59	29.66
21	25.83	28.68	29.18	29.41	29.49
22	25.93	28.71	29.21	29.46	29.52
23	25.89	28.59	29.06	29.30	29.36
24	25.76	28.29	28.72	28.96	29.02
25	25.94	28.58	29.08	29.33	29.38
26	25.95	28.63	29.09	29.37	29.42
27	25.92	28.47	28.92	29.18	29.24
28	25.76	28.39	28.84	29.10	29.17
29	25.86	28.38	28.84	29.09	29.16
30	26.05	28.63	29.13	29.40	29.49
Average	26.82	29.47	29.95	30.21	30.27

proposed algorithm achieves a better quality of interpolated images than the conventional interpolation methods. We also compare the computation time for the interpolation methods. The programs are performed using C++ language and complied using the Microsoft Visual C++ package. All simulations are made on a single-CPU Intel Pentium III-1 GHz personal computer with the Windows XP operating system. Table 3 shows

Table 3 The average execution time (t_e) and the average learning time (t_l) of the interpolation schemes

	Bilinear	Cubic	WMI_{LL}	WMI	SMI
t_e (ms)	10	160	28	71	213
t_l (s)	–	–	24	77	80

the average execution time and the average learning time for the test images. Notice that t_e (execution time) is evaluated for the images outside the training set and t_l (learning time) is evaluated for the images inside the training set. The magnified portions of the interpolated images "Lena" outside the training set are shown in Fig. 5a–e. It can be easily seen that the proposed algorithm can obtain the better image quality and the better visual quality about the edge region. Figure 6a, g are the original low-resolution frames 10 and 20 of the "Football" sequence, respectively. Figure 6b–f and h–l are the interpolated images for the low-resolution frames 10 and 20 using the Bilinear, Cubic, SMI, WMI_{LL}, and WMI methods. To show the differences clearly, the portion in the original low-resolution image and the interpolated images "F-16" that contain some fine texts are given in Fig. 7a–d. Besides, the difference between the original high-resolution image and the interpolated images that are generated by the Cubic and WMI algorithm are shown in Fig. 8a, b, respectively. In all simulation results, the images resulting from the interpolation with the new algorithm using wavelet reconstruction obtains the better image quality and faster computation than those obtained with other approaches.

5 Conclusions

In this paper, we proposed an efficient scheme for digital image interpolation. The proposed algorithm increases the resolution of a low-resolution image by using neural networks. In order to estimate the inter-

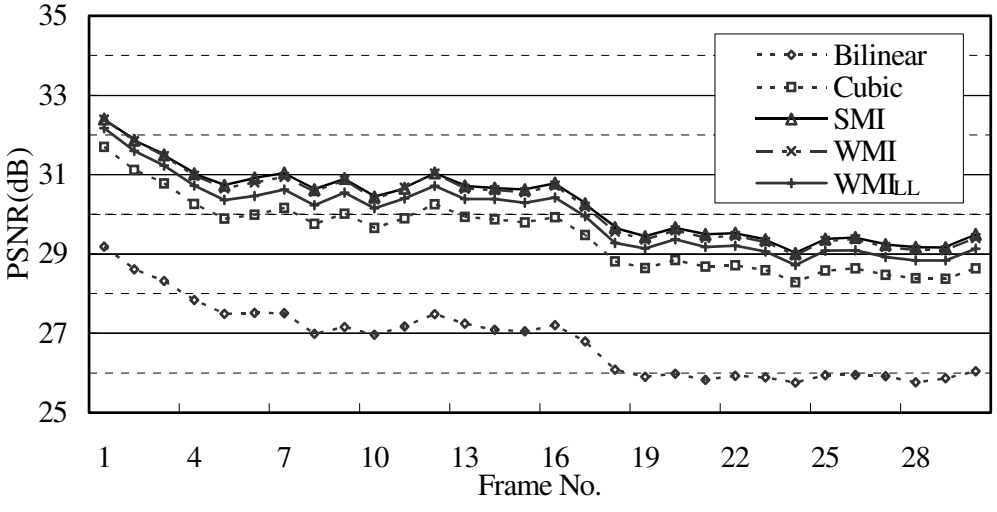

Fig. 4 The simulation results for the interpolated images of the "Football" sequence with resolution increasing by a factor of two

Fig. 5a–e The magnified portions of the interpolated image "Lena." **a** Bilinear. **b** Cubic. **c** WMI_{LL}. **d** WMI. **e** SMI

polated image more accurately, the WMI scheme adopts the MLP class of neural networks to predict the expected wavelet sub-images of a high-resolution image. The back-propagation learning algorithm is used to construct the synaptic weights for the MLP predictors. The wavelet analysis/synthesis procedure and MLP can be implemented easily by using very large scale integration (VLSI) techniques. Thus, the hardware design for the proposed interpolation schemes is simple and efficient. From the experimental results, the proposed schemes can obtain superior image quality and visual quality about the edge region. We find that the proposed schemes are expected to be useful interpolation schemes for digital images.

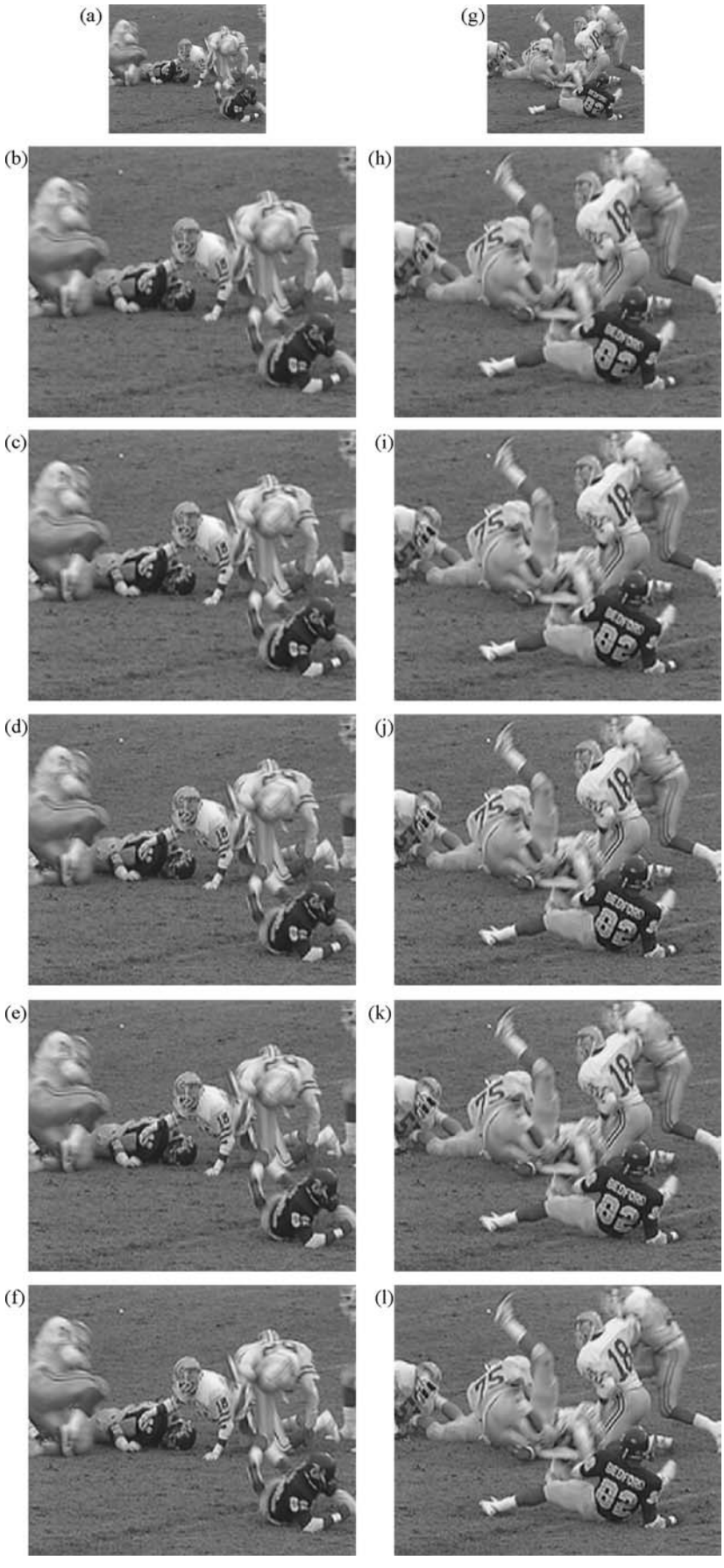

Fig. 6a–l Interpolation results for the images of the "Football" sequence. **a** and **g** Original frames 10 and 20. **b** and **h** Bilinear. **c** and **i** Cubic. **d** and **j** WMI_{LL}. **e** and **k** WMI. **f** and **l** SMI

Fig. 7a–d The magnified portions of the reconstructed images "F-16." **a** Low-resolution image. **b** Interpolated by Cubic. **c** Interpolated by WMI_{LL}. **d** Interpolated by WMI

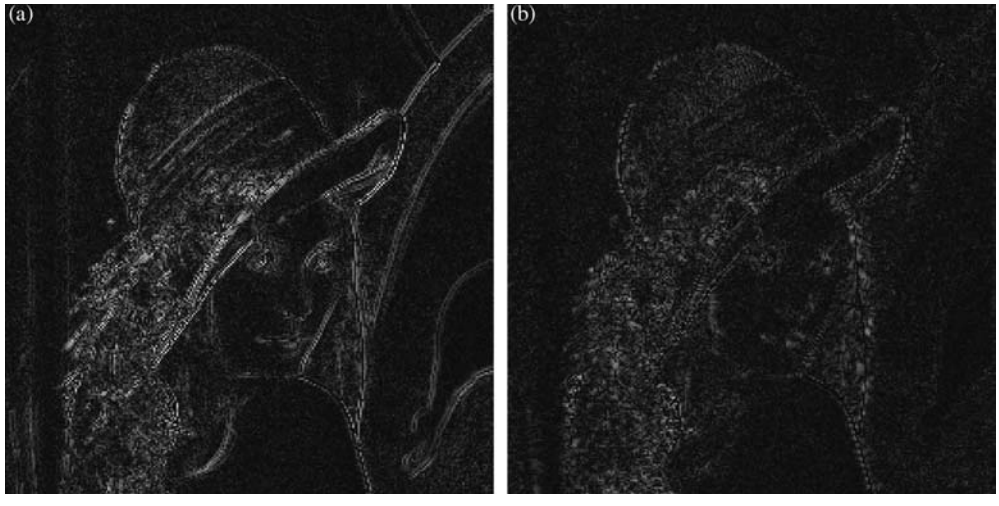

Fig. 8a, b Results of the difference between the original image and reconstructed image "Lena." **a** Interpolated by Cubic. **b** Interpolated by WMI

Acknowledgements This work was supported by the National Science Council, Taiwan, Republic of China, under Grant NSC-91–2213-E-029–021.

References

1. Hou H, Andrews H (1978) Cubic splines for image interpolation and digital filtering. IEEE Trans Acoust Speech (ASSP) 26(6):508–517
2. Keys RG (1981) Cubic convolution interpolation for digital image processing. IEEE Trans Commun 29(6):1153–1160
3. Han JK, Baek S-U (2000) Parametric cubic convolution scaler for enlargement and reduction of image. IEEE Trans Consumer Electron 46(2):247–256
4. Reichenbach SE, Geng F (2003) Two-dimensional cubic convolution. IEEE Trans Image Processing 12(8):857–865
5. Zeng B, Venetsanopoulos AN (1998) Image interpolation based on median-type filters. Opt Eng 37(9):2472–2482
6. Jensen K, Anastassiou D (1995) Subpixel edge localization and the interpolation of still images. IEEE Trans Image Processing 4(3):285–295
7. Hong KP, Paik JK, Kim HJ, Lee CH (1996) An edge-preserving image interpolation system for a digital camcorder. IEEE Trans Consumer Electron 42(3):279–284

8. Hao J, Moloney C (2002) A new direction adaptive scheme for image interpolation. In: Proceedings of the IEEE international conference on image processing (ICIP 2002), Rochester, New York, September 2002 3:369–372
9. Xiqun L, Hong PS, Smith A (2003) An efficient directional image interpolation method. In: Proceedings of the IEEE international conference on acoustics, speech, and signal processing (ICASSP 2003), Hong Kong, April 2003 3:97–100
10. Qing W, Ward R (2003) A contour-preserving image interpolation method. In: Proceedings of the IEEE international conference on image processing (ICIP 2003), Barcelona, Spain, September 2003 3:673–676
11. Darwish AM, Bedair MS, Shaheen SI (1997) Adaptive resampling algorithm for image zooming. IEE Proc Vis Image Signal Process 144(4):207–212
12. Chang SG, Cvetkovic Z, Vetterli M (1995) Resolution enhancement of images using wavelet transform extrema extrapolation. In: Proceedings of the IEEE international conference on acoustics, speech, and signal processing (ICASSP'95), Detroit, Michigan, May 1995 4:2379–2382
13. Carey WK, Chuang DB, Hemami SS (1999) Regularity-preserving image interpolation. IEEE Trans Image Processing 8(9):1293–1297
14. Plaziac N (1999) Image interpolation using neural networks. IEEE Trans Image Process 8–11:1647–1651
15. Dumitras A, Kossentini F (1998) FAAN-based video chrominance subsampling. In: Proceedings of the IEEE international conference on acoustics, speech, and signal processing (ICASSP'98), Seattle, Washington, May 1998 2:1077–1080
16. Kim JO, Choi BT, Morales A, Ko SJ (1999) Neural concurrent subsampling and interpolation for images. In: Proceedings of the IEEE region 10 conference (TENCON'99), Cheju, Korea, September 1999 2:1327–1330
17. Grossberg ES (1988) Neural networks and natural intelligence. MIT Press, Cambridge, Massachusetts
18. Haykin S (1994) Neural networks. Macmillan, New York
19. Masters T (1994) Signal and image processing with neural networks. Wiley, New York
20. Lippman RP (1987) An introduction to computing with neural nets. IEEE ASSP Mag 4:4–22
21. Averbuch A, Lazar D, Israeli M (1996) Image compression using wavelet transform and multiresolution decomposition. IEEE Trans Image Processing 5(1):4–15
22. Rumelhart DE (1986) Parallel distributed processing. MIT Press, Cambridge, Massachusetts
23. Nielsen RH (1989) Theory of the back-propagation neural network. In: Proceedings of the international joint conference on neural networks, Washington, DC, June 1989 1:593–606
24. Hirose Y, Yamashita K, Hijiva S (1991) Back-propagation algorithm which varies the number of hidden units. Neural Netw 4(1):61–66
25. Chui CK (1992) An introduction to wavelets. Academic, Boston, Massachusetts
26. Mallat SG (1989) A theory for multiresolution signal decomposition: the wavelet representation. IEEE Trans Pattern Anal Mach Intell (PAMI) 11(7):647–693
27. Hammerstron D (1990) A VLSI architecture for high-performance, low-cost, on-chip learning. In: Proceedings of the international joint conference on neural networks, Washington, DC, June 1990 2:537–544
28. Hammerstron D (1992) Electronic neural network implementation. In: Proceedings of the international joint conference on neural networks, Baltimore, Maryland, June 1992, tutorial 5
29. Säckinger E, Boser BE, Bromley J, LeCun Y, Jackel LD (1992) Application of the ANNA neural network chip to high-speed character recognition. IEEE Trans Neural Netw 3:498–505
30. Antonini M, Barlaud M, Mathieu P, Daubechies I (1992) Image coding using wavelet transform. IEEE Trans Image Processing 1(2):205–220
31. Johnston JD (1980) A filter family designed for use in quadrature mirror filter banks. In: Proceedings of the IEEE international conference on acoustics, speech, and signal processing (ICASSP'80), Denver, Colorado, April 1980, pp 291–294